

Fast response 2×2 thermo-optic switch with polymer/silica hybrid waveguide

Yunfei Yan (闫云飞), Chuantao Zheng (郑传涛), Xiaoqiang Sun (孙小强),
Fei Wang (王菲), and Daming Zhang (张大明)*

State Key Laboratory on Integrated Optoelectronics, College of Electronic Science and Engineering,
Jilin University, Changchun 130012, China

*Corresponding author: zhangdm@jlu.edu.cn

Received February 9, 2012; accepted March 14, 2012; posted online May 16, 2012

A polymer/silica hybrid 2×2 multimode-interference Mach-Zehnder interferometer thermo-optic (TO) switch is designed and fabricated. Instead of polymer, silica is used as under-cladding to accelerate heat release because of its large thermal conductivity. The developed switch exhibits low power consumption of 6.2 mW, low crosstalk of about -28 dB, and short response time. The rise and fall times of 103 and 91 μs for this hybrid switch are shortened by 40.8% and 52.4%, respectively, compared with those of the fabricated TO switch (174 and 191 μs) using polymer as both upper- and under-claddings.

OCIS codes: 250.6715, 250.5460, 160.6840.

doi: 10.3788/COL201210.092501.

Optical switches as well as other coplanar lightwave devices play an important role in optical communication networks^[1,2]. The thermo-optic (TO) ones are attractive for their small size, large scalability, and stability in long-term operation. Two material systems, namely, silica/silicon and polymer, are adopted in the design and fabrication of the TO switch. The silica/silicon one has a faster response speed because of the large thermal conductivity of silicon and the small device height. A silica/silicon TO switch with fast response time of about 700 ns has been reported^[3]. However, it requires hundreds of milliwatts of driving power. Shoji *et al.* reported a silicon nanowire waveguide TO switch with 40-mW power consumption and 30- μs response time^[4]. Previous studies have investigated the suspended waveguide structure with the aim of reducing power consumption^[5,6]. However, the fabrication process and technology have become extremely complicated. The polymer one has lower power consumption and simple fabrication technology. Polymer multimode-interference (MMI) Mach-Zehnder interferometer (MZI) TO switches with power consumption of as low as 1.85 mW^[7] and short response time of less than 0.2 ms^[8] have been reported. Using direct ultraviolet photolithography, we fabricated a polymer TO switch exhibiting 7.5 mW of power consumption and 0.4 ms of response time^[9].

In this letter, a 2×2 TO switch based on the MMI-MZI structure is realized. To improve the switch response performance, we adopt a polymer/silica hybrid waveguide. Fabricated via direct ultraviolet photolithography and wet etching, the switch expresses high-speed response and low power consumption.

As shown in Fig. 1, the TO switch is designed based on the MZI structure with a 3-dB MMI splitter and coupler. It uses a silicon substrate, which is a good heat sink. In the heater region, a thin-film heater is utilized to change the mode refractive index and propagation characteristic in the waveguide. Silica has larger thermal conductivity (about $1.4 \text{ WK}^{-1}\text{m}^{-1}$) compared with polymer. Thus, it is used as the under cladding to obtain faster re-

sponse. SU-8 (commercially from MicroChem), which has a high TO coefficient of about $-1.8 \times 10^{-4} \text{ K}^{-1}$, is used to form the waveguide core. The synthesized material poly(methyl methacrylate) (PMMA) is used as the upper cladding. The indices of the core, under cladding, and upper cladding are 1.573, 1.46, and 1.483, respectively, at 1550-nm wavelength. The contrast between the refractive indices of PMMA and SU-8 is high. Thus, a relatively thin upper cladding can be used to confine the optical mode field. The mode is calculated using the beam propagation method (BPM), and the optical mode distribution is shown in Fig. 2(a). For a single-mode waveguide, the core width and height are both confined at 2.5 μm . Moreover, the length of the MMI region is optimized to 278 μm to realize a 3-dB splitter and coupler. As shown in Fig. 3, half of an input optical signal, which propagates from input fiber 1, is coupled to the waveguide in the upper path (path 1). The other half is coupled to the lower path (path 2). When no driving power is applied on the heater, the optical power will output from the end of path 2 and couple with output fiber 2. This state is called "cross state". When appropriate power is applied on the heater, the π -phase difference between two beams is produced. However, the optical power will couple with output fiber 1 because of the interference in the direction coupler. This state is called "bar state".

The steady-state response evaluation of the device is conducted by solving the following heat transfer

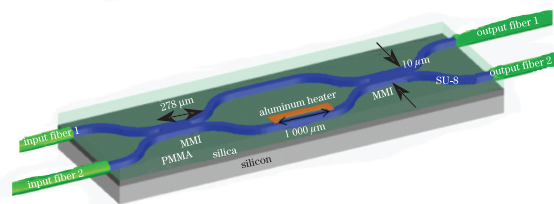


Fig. 1. Schematic diagram of the polymer/silica hybrid MMI-MZI TO switch.

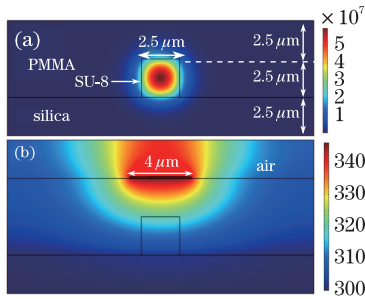


Fig. 2. Cross section of the switch: (a) Optical and (b) heat distributions.

equation^[8]:

$$\rho c_p \frac{\partial T}{\partial t} = k \nabla^2 T + Q(x, y, z, t), \quad (1)$$

where T is the temperature, $Q(x, y, z, t)$ is the heat generation rate per unit volume, ρ is the material density, c_p is the heat capacity, and k is the thermal conductivity. The initial temperature is assumed to be $T(x, y, z, t) = 300$ K and the boundary conditions are $\nabla T = -h(T - T_A)$ on the top surface, $T = 300$ K on the bottom surface, $k_1 \nabla T_1 - k_2 \nabla T_2 = 0$ on internal boundaries, where h is the natural convection heat transfer coefficient and T_A is the air temperature. According to the material parameters in Table 1, the steady-state thermal distribution in the active waveguide is calculated and drawn in Fig. 2(b). The power switching is simulated using BPM software and shown in Fig. 4(b). When the power is set to 6.1 mW, the switch shifts to “bar state” from “cross state”, and the average temperature of the core layer under the heater increases to 304.45 K.

The switch transient characteristics are also simulated. The switching time is defined as the time needed to reach $(1 - 1/e)$ of the steady-state temperature^[10]. Furthermore, we calculate the switching times of the devices using two different materials, namely, silica and PMMA, as under cladding. The results are shown in Fig. 4(a). The switching time of the silica/polymer hybrid switch ($108 \mu\text{s}$) is much shorter than that of the polymer switch ($180 \mu\text{s}$). The three layers can be approximately seen as equivalent layers with the effective thermal conductivity k_{eff} , density ρ_{eff} , and heat capacity $c_{p\text{eff}}$. The switching time τ can be determined by $\tau = 0.47L^2/\gamma$ ^[10], where L is the slab thickness and $\gamma = k_{\text{eff}}/\rho_{\text{eff}}c_{p\text{eff}}$. The switching time τ is proportional to the square of the slab thickness L^2 and inversely proportional to the effective thermal conductivity k_{eff} . A smaller L and a larger k_{eff} are both useful to obtain faster response. Therefore, the reduced upper-/under-cladding thickness allows the heat flux toward the substrate in a shorter distance. The thermal conductivity of silica is

Table 1. Parameters of Adopted Materials

Material	ρ (kg/m ³)	C_p (J/kg·K)	k (W/mK)
SU-8	1 190	1 200	0.2
PMMA	1 190	1 420	0.19
Silica	2 200	730	1.4
Silicon	2 330	703	163

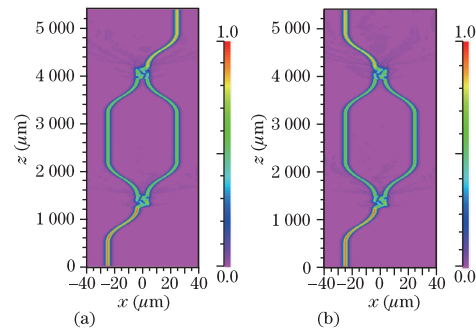


Fig. 3. Simulated optical distributions in (a) cross and (b) bar states.

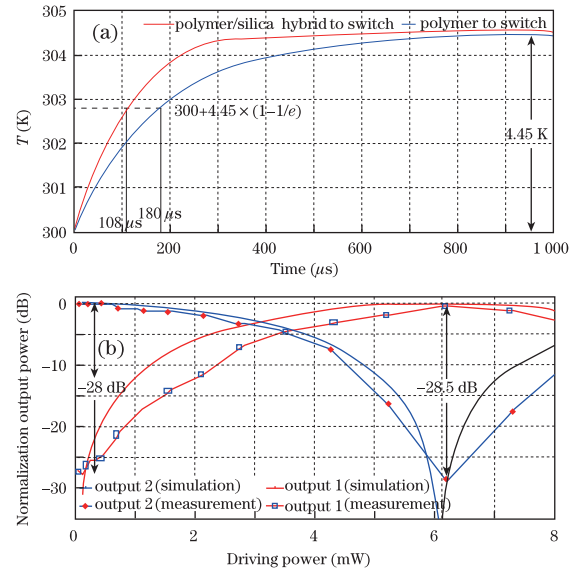


Fig. 4. (a) Simulated average temperature variation in the core under the heater region response to time. (b) Measured and simulated curves of output power versus driving power (the light is launched into the switch from input fiber 1).

six times larger than that of PMMA. Hence, using silica as under-cladding is beneficial in accelerating the heat transfer from the core to the substrate.

For the under-cladding, a $2.5\text{-}\mu\text{m}$ -thick silica layer was grown on the silicon substrate using thermal oxide. For the core, a $2.5\text{-}\mu\text{m}$ -thick SU-8 layer was spin-coated on the under-cladding. The waveguide was formed via photolithography, wet etching, and soft bake processes. Then, the film was hard baked to realize sufficient cross-link and obtain stable chemical and thermal properties. The waveguide core configuration is characterized using a scanning electron microscope (SEM), and the results are shown in Fig. 5. Finally, PMMA was spin-coated to form the upper cladding.

A 100-nm -thick aluminum layer was deposited on top of the upper cladding via thermal evaporation. The heater was patterned via conventional photolithography and wet etching.

For the measurements, an input power (1 mW at 1550 nm) from input single-mode fiber 1 was coupled with the switch. The insertion loss, including the coupler, transmission, and excess losses, was less than 9.8 dB. The relative output power was obtained when driving

power was applied. The result is shown in Fig. 4(b). We obtained a slightly larger measured switching power (6.2 mW) compared with the simulation result. The crosstalk values at the cross and bar states were -28 and -28.5 dB, respectively. A square wave signal was used to drive the switch, and the dynamic performance was expressed by the rise and fall times of 103 and 91 μs , as shown in Fig. 6. To confirm the advantages of the polymer/silica hybrid structure, we fabricated and measured a polymer TO switch with PMMA under cladding. The rise and fall times were 174 and 191 μs , respectively. The comparison is shown in Table 2. Therefore, using a polymer/silica hybrid structure reduces the response time by more than 40% relative to the polymer switch.

The performances of this fabricated TO switch are also compared with those of the other reported TO

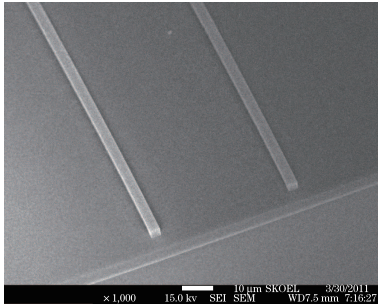


Fig. 5. Fabricated waveguide core characterized by SEM.

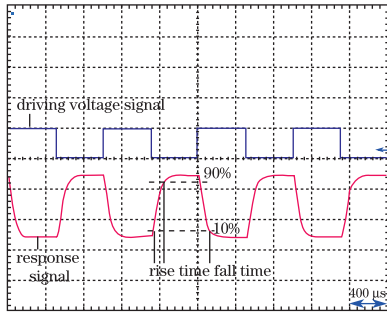


Fig. 6. Switching response on a rectangular wave.

Table 2. Comparison Between the Performances of the Polymer/Silica Hybrid and Polymer Switches

Waveguide	Polymer/Silica	All-Polymer	Reduction
Rise Time (μs)	103	174	40.8%
Fall Time (μs)	91	191	52.4%

Reduction is obtained from $R_{\text{rise}} = \frac{T_{\text{rise}}^{\text{P}} - T_{\text{rise}}^{\text{h}}}{T_{\text{rise}}^{\text{P}}}$ and $R_{\text{fall}} = \frac{T_{\text{fall}}^{\text{P}} - T_{\text{fall}}^{\text{h}}}{T_{\text{fall}}^{\text{P}}}$, where $T_{\text{rise}}^{\text{h}}$ and $T_{\text{fall}}^{\text{h}}$ are the rise and fall time of the hybrid switch, respectively, and $T_{\text{rise}}^{\text{P}}$ and $T_{\text{fall}}^{\text{P}}$ are the rise and fall time of the polymer switch, respectively.

switches^[5–7]. At the same level of power consumption, the hybrid TO switch exhibits a much faster response time and larger crosstalk.

Although the rise and fall time of this hybrid switch are shortened, they are still much longer than those of the SOI switch. To improve the response performance further, one can decrease the thicknesses of the core and cladding layers as much as possible by ensuring single-mode propagation and low optical loss. Moreover, to shorten the heat dispatch/transfer time, one can use materials with larger thermal conductivities than that of the polymer upper cladding in this letter.

In conclusion, a polymer/silica hybrid TO switch based on the MMI-MZI structure is designed and fabricated. Owing to the larger TO coefficient of polymer and larger thermal conductivity of silica, the switch exhibits a faster response time (rise and fall times are 103 and 91 μs , respectively), which is 40% shorter than that of the switch using polymer as upper- and under-claddings. The proposed switch also exhibits a low switching power of 6.2 mW

This work was supported by the National Natural Science Foundation of China (Nos. 61077041, 61107021, and 61177027), the Ministry of Education of China (Nos. 20110061120052 and 20090061110041), the China Post-doctoral Science Foundation (No. 20110491299), and the Special Funds of Basic Science and Technology of Jilin University (Nos. 200905005, 201100253, and 201103076).

References

1. J. Li, J. An, Y. Wu, J. Li, H. Wang, and X. Hu, *Chin. Opt. Lett.* **8**, 588 (2010).
2. X. Xiao, H. Xu, L. Zhou, Z. Li, Y. Li, Y. Yu, and J. Yu, *Chin. Opt. Lett.* **8**, 757 (2010).
3. M. Harjanne, M. Kapulainen, T. Aalto, and P. Heimala, *IEEE Photon. Technol. Lett.* **16**, 2039 (2004).
4. Y. Shoji, K. Kintaka, S. Suda, H. Kawashima, T. Hasama, and H. Ishikawa, *Opt. Express* **18**, 9071 (2010).
5. Q. Fang, J. F. Sun, T.-Y. Liow, H. Cai, M. B. Yu, G. Q. Lo, and D.-L. Kwong, *IEEE Photon. Technol. Lett.* **23**, 525 (2011).
6. K. Watanabe, Y. Hashizume, Y. Nasu, M. Kohtoku, M. Itoh, and Y. Inoue, *J. Lightwave Technol.* **26**, 2235 (2008).
7. A. M. Al-hetar, A. B. Mohammad, A. S. M. Supa'at, Z. A. Shamsan, and I. Yulianti, *Opt. Commun.* **284**, 1181 (2011).
8. N. Xie, T. Hashimoto, and K. Utaka, *IEEE Photon. Technol. Lett.* **21**, 1861 (2009).
9. L. Gao, J. Sun, X. Sun, C. Kang, Y. Yan, and D. Zhang, *Opt. Commun.* **282**, 4091 (2009).
10. G. Coppola, L. Sirleto, I. Rendina, and M. Iodice, *Opt. Eng.* **50**, 071112 (2011).